DOI: 10.1002/ejic.200700658

Evidence for Ligand-Centered Reactivity of a 17e Radical Cationic 2*H*-Azaphosphirene Complex

Holger Helten,[a] Christoph Neumann,[b] Arturo Espinosa,[c] Peter G. Jones,[b] Martin Nieger,[d] and Rainer Streubel*[a]

Keywords: Ligand-centered reactivity / Phosphorus heterocycles / Electron transfer

Reactions of 2*H*-azaphosphirene complex **1** with electron-rich nitrile derivatives **2a–e** in the presence of substoichiometric amounts of ferrocenium hexafluorophosphate yielded regioselectively 2*H*-1,4,2-diazaphosphole complexes **3a–e** under mild conditions. The dependence of the reaction on the amount of ferrocenium hexafluorophosphate is discussed. In the reactions of **1** with electron-poor nitrile derivatives HCN (**2f**), EtOC(O)CN (**2g**), and C_6F_5CN (**2h**), byproducts possessing a P–F bond are formed, which indicates that the hexafluorophosphate anion is involved in the reaction course. Apart from NMR spectroscopic (**3a–f**) and X-ray data (**3b**, **3d–e**), a detailed DFT study is included that provides first insight into the reaction pathway.

Introduction

The generation of radical cationic intermediates has emerged as a useful synthetic tool in organic[1–4] and organometallic chemistry.[5] Oxidation of closed-shell organic molecules by single-electron transfer (SET) results in strongly destabilized odd-electron species that very often tend to fragment. Thus, upon pulse radiolysis or ^{60}Co γ radiolysis, phenylaziridines either form transient radical cations with retention of the closed ring structure or undergo ring opening with formation of radical cationic azomethine ylides depending on their substitution patterns.[6] Although the spin density of most organometallic radicals is localized mainly at the metal center, organometallic radicals can show both metal-centered and/or ligand-centered reactivity, whereas 17e cationic complexes often show the latter behavior.[7] For the generation of radical cations in solution four major routes are currently in use: (1) anodic oxidation, (2) photoinduced electron transfer (PET), (3) oxidation by radicals generated by pulse or γ radiolysis, and (4) chemical oxidation.[1,2] In this work, ferrocenium salts are used as mild single-electron oxidants, which have the further advantage that they are more easily recycled than most other heavy metal oxidants. Ferrocenium salts have been successfully applied in organic[8] and organometallic syntheses.[5] Recently, they were employed in the oxidation of N-heterocyclic carbenes.[9]

In the course of our studies concerning the applicability of 2*H*-azaphosphirene metal complexes **I**[10] (Scheme 1) in heterocyclic ligand syntheses,[11] we discovered that **I** undergoes P–N bond-selective ring-expansion reactions in the presence of substoichiometric amounts of typical single-electron oxidants such as tetracyanoethylene[12] and/or ferrocenium hexafluorophosphate.[13]

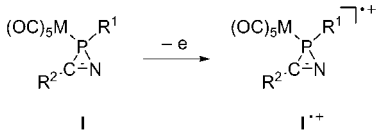

I I•+

Scheme 1. 2*H*-Azaphosphirene complexes **I** and radical cationic 2*H*-azaphosphirene complexes $\mathbf{I}^{\bullet+}$ (M = Cr, Mo, W; R^1, R^2 = ubiquitous organic substituents).

Preliminary studies showed that these reactions require polar solvents such as dichloromethane or carbonitriles, reactants with a π system having a lone pair of electrons at one terminus, and substituents that are not (too) bulky. In all ferrocenium hexafluorophosphate induced ring expansions, the formation of small amounts of ferrocene is observed,[13b,13c] which indicates the transient formation of radical cationic species such as $\mathbf{I}^{\bullet+}$ (Scheme 1). Further evidence for the intermediate formation of $\mathbf{I}^{\bullet+}$ was obtained by the finding that reaction rates are reduced if *ortho*-phenyl-

[a] Institut für Anorganische Chemie, Rheinische Friedrich-Wilhelms-Universität Bonn,
Gerhard-Domagk-Strasse 1, 53121 Bonn, Germany
Fax: +49-228-73-9616
E-mail: r.streubel@uni-bonn.de
[b] Institut für Anorganische und Analytische Chemie der Technischen Universität Braunschweig,
Postfach 3329, 38023 Braunschweig, Germany
[c] Departamento de Química Orgánica, Facultad de Química, Universidad de Murcia,
Campus de Espinardo, 30100 Murcia, Spain
[d] Laboratory of Inorganic Chemistry, Department of Chemistry, University of Helsinki,
P. O. Box 55 (A.I. Virtasen aukio 1), 00014 Helsinki, Finland
Supporting information for this article is available on the WWW under http://www.eurjic.org or from the author.

substituted 2*H*-azaphosphirene complexes with electron-donating substituents were employed.[13b] Despite all these indications, fundamental questions remained open regarding reaction pathways, for example, at which stage does the three-membered ring open and/or do transition-metal coordination spheres increase during the reactions.

Here, reactions of 2*H*-azaphosphirene complex **1** with nitriles of varying donor abilities under SET conditions are reported. A detailed DFT study on the reaction pathway is included.

Results and Discussion

Reactions of 2*H*-azaphosphirene complex **1**[10] with dimethylcyanamide (**2a**) and electron-rich five-membered heterocyclic nitrile derivatives RCN (**2b**–**e**; Scheme 2) in the presence of substoichiometric amounts (0.05 equiv.) of ferrocenium hexafluorophosphate ([FcH]PF_6) at ambient temperature regioselectively yielded 2*H*-1,4,2-diazaphosphole complexes **3a**–**e** (Scheme 2). The molecular structures of **3a**–**e** were unambiguously established by multinuclear NMR spectroscopic experiments and mass spectrometry.

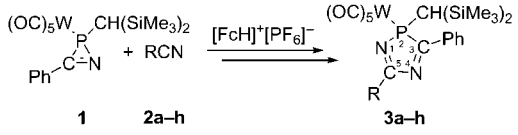

Scheme 2. Synthesis of 2*H*-1,4,2-diazaphosphole complexes **3a**–**h** (**a**: R = NMe_2; **b**: R = 1,5-dimethyl-2-pyrryl; **c**: R = 2-furyl; **d**: R = 2-thienyl; **e**: R = 3-thienyl; **f**: R = H; **g**: R = CO_2Et; **h**: R = C_6F_5).[14]

We monitored the ring expansion reaction of **1** + **2d** → **3d** (Scheme 2) at different concentrations of [FcH]PF_6 by using $^{31}P\{^1H\}$ NMR spectroscopy (Figure 1). These series revealed that the reaction progression depends strongly on the amount of [FcH]PF_6, but it can be reduced to 0.03 equiv. (0.01 mol L^{-1}) without a significant decrease in the conversion. If only 0.02 equiv. of [FcH]PF_6 was used, the conversion leveled off at around 80%; in the presence of 0.01 equiv. of [FcH]PF_6 even after 3 d the ratio of **3d** did not exceed 18%, and in the absence of [FcH]PF_6 no conversion of **1** was detected within 10 d (not shown). For ratios ≥0.02 equiv. of [FcH]PF_6, the curves show a steep ascending slope after a comparably flat trend at the start, and again a flattening at the end. As no resonances other than those of **1** and **3d** were detected by $^{31}P\{^1H\}$ NMR spectroscopic monitoring during the reaction course, the time dependent decrease of **1** follows the same trend as the increase of **3d**. Because we were interested in understanding the start of the reaction, we decided to monitor the reaction of **1** with **2d** with 0.025 equiv. of [FcH]PF_6 at more frequent time intervals (Figure 2).

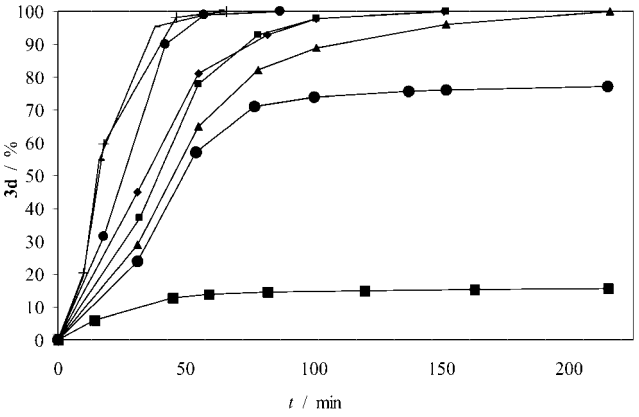

Figure 1. Ratio of **3d** over reaction time for the reaction of **1** with **2d** in the presence of varying amounts of [FcH]PF_6: ■ 0.01, ● 0.02, ▲ 0.03, ■ 0.04, ♦ 0.05, · 0.10, + 0.15, - 0.20 equiv.

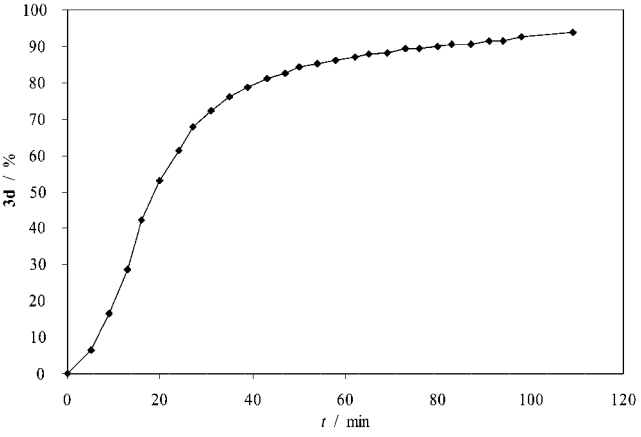

Figure 2. Ratio of **3d** over reaction time for the reaction of **1** with **2d** in the presence of 0.025 equiv. of [FcH]PF_6. The reaction is complete after 1 d.

The flat trend at the start is quite obvious. The fastest increase in the amount of **3d** is recorded between 29 and 42% conversion. It should be noted that a flat trend at the start of the reaction is characteristic for autocatalytic reactions, and in reactions with a very low starting concentration of the autocatalytic species the peak of the reaction rate is recorded at around 50% conversion.[15]

On the basis of these results and the finding that ferrocene is formed during the reaction, we suppose a radical cation chain reaction mechanism initiated by oxidation of **1** by the ferrocenium cation with formation of radical cation $\mathbf{1}^{\cdot+}$ and ferrocene (Scheme 3).[16]

The observed acceleration in the reaction rate at the start (Figures 1 and 2) can be explained by assuming slow oxidation of **1** followed by a fast ring-expansion reaction of highly reactive radical cation $\mathbf{1}^{\cdot+}$ with nitrile **2a**–**e**. The cycle is closed by reduction of radical cationic 2*H*-1,4,2-diazaphosphole complexes $\mathbf{3}^{\cdot+}$**a**–**e** by **1** to yield **3a**–**e** and $\mathbf{1}^{\cdot+}$, which then can restart the chain reaction. In consequence, the generation of $\mathbf{1}^{\cdot+}$ causes its multiplication, and it may be regarded as the autocatalytic species of this cycle. If

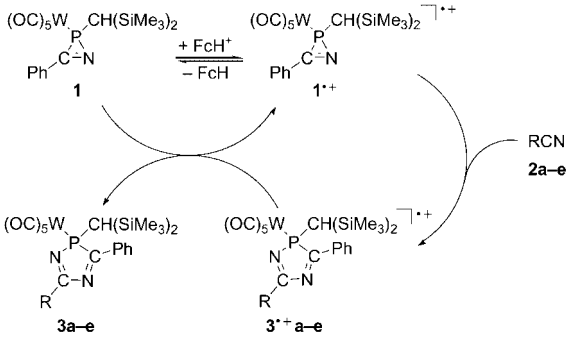

Scheme 3. Proposed chain reaction of 2*H*-azaphosphirene complex **1** with nitrile derivatives **2a**–**e** initiated by the ferrocenium cation $[FcH]^+$.

0.02 equiv. of $[FcH]PF_6$ was employed (Figure 1), the chain reaction was terminated at some point. Obviously, 0.01 equiv. of $[FcH]PF_6$ is not sufficient for the successful initiation of the chain reaction (Figure 1).

In contrast to **2a**–**e**, the reaction of **1** with HCN (**2f**) proceeded much more slowly and was unselective. Reaction monitoring showed that even after a short time (1.5 h) a variety of ^{31}P NMR spectroscopic resonances was detected, including a resonance at δ = 105.5 ppm (Table 1) with a tungsten–phosphorus coupling constant of 225.1 Hz and a phosphorus–hydrogen coupling constant of 34.3 Hz, which revealed the formation of **3f** (ca. 16%). Even though an excess of **2f** (2.6 equiv.) was employed, after 4 d the reaction solution still contained 16% (ratio estimation by $^{31}P\{^1H\}$ NMR spectroscopic resonance integration) of unreacted **1** and only 20% of **3f**, besides numerous unidentified byproducts. Some of the latter showed large phosphorus–fluorine coupling constants (see Experimental Section), thus revealing that the hexafluorophosphate anion, which is usually regarded as weakly coordinating, had taken part in the reaction course. As reported recently, highly electrophilic cationic species are able to abstract fluoride from the hexafluorophosphate anion.[17] Byproducts bearing a P–F bond were also found in the reaction of **1** with electron-poor nitrile derivative **2g** (see below and Experimental Section). After 6 d, 41% of **1** remained unreacted, and a product with a ^{31}P NMR spectroscopic resonance at δ = 110.7 ppm (21%) was observed that featured a tungsten–phosphorus coupling constant of 227.6 Hz. These data are too close to those of **3b**–**e** and, therefore, an assignment to **3g** is not supported; even more vexing is the finding that in the reaction of **1** with **2f** a byproduct having analogous $^{31}P\{^1H\}$ NMR spectroscopic data was detected. Reaction of **1** with **2h** showed a similar behavior to that of **1** with **2g**, and again, a product with a ^{31}P NMR spectroscopic resonance at δ = 110.7 ppm with a tungsten–phosphorus coupling constant of 228.9 Hz was observed (12% after 6 d) as well as numerous byproducts, some of which showed large phosphorus–fluorine coupling constants (see Experimental Section). Even after 6 d, 48% of **1** − and the entire amount of **2h** [by $^{19}F\{^1H\}$ NMR spectroscopy] − remained unreacted, thus indicating that **2h** had not reacted at all even though an excess of 6.4 equiv. was employed. The $^{19}F\{^1H\}$ NMR spectroscopic resonance of the hexafluorophosphate anion decreased in the course of the reaction, and after 6 d its $^{31}P\{^1H\}$ NMR spectroscopic resonance was no longer detected.

Table 1. $^{31}P\{^1H\}$ NMR spectroscopic data of **3a**–**f**.

	3a[a]	**3b**[a]	**3c**[a]	**3d**[a]	**3e**[a]	**3f**[b]
δ / ppm	102.1	108.4	110.6	110.5	109.1	105.5
$^1J_{W,P}$ / Hz	240.3	233.9	230.6	229.5	229.8	225.1

[a] In $CDCl_3$. [b] In CH_2Cl_2.

The $^{31}P\{^1H\}$ NMR spectroscopic data of **3b**–**e**, displayed in Table 1, are similar, and each complex has a resonance at about 110 ppm. Concerning the magnitudes of the tungsten–phosphorus coupling constant, a definite trend can be seen: $^1J_{W,P}$ constants increase with increasing donor ability[18] of the substituent at C-5 in the order: 3-thienyl ≈ 2-thienyl < 2-furyl < 1,5-dimethyl-2-pyrryl. The tungsten–phosphorus coupling constant of complex **3a**, which has a very strong electron-donating substituent (NMe_2) attached to C-5, is about 6 Hz larger than that of complex **3b**, whereas the ^{31}P NMR spectroscopic resonance is shifted by around 6 ppm to higher field. Consequently, the smallest tungsten–phosphorus coupling constant ($^1J_{W,P}$ = 225.1 Hz) was exhibited by complex **3f**, which has no substituent in the C-5 position, which lends further support to the assignment made beforehand. A further consequence can be expected from this trend: for **3g** and **3h** even lower values are expected.

To examine the aforementioned formation of products with a P–F bond, we investigated the role of the counteranion. In the reaction of **1** with **2d** we exchanged hexafluorophosphate for the weaker nucleophilic counteranion tetraphenylborate, which could not serve as a fluoride source. The outcome was a clean reaction yielding complex **4d** (by ^{31}P NMR spectroscopy), which also indicated that the counteranion did not play a crucial role for the ring expansions of **1** as induced by ferrocenium salts. So, the products bearing a P–F bond in the reaction of **1** with **2f** and **2g** do not constitute intermediates of the ring-expansion reaction pathway. Instead, these should be regarded as byproducts emerging from the reaction of transiently formed highly electrophilic species with hexafluorophosphate through fluoride transfer. To elucidate further the effect that $[FcH]BPh_4$ might have on reactions of **1**, we looked again at the reactions with electron-poor nitrile derivatives **2f**–**h** by using this SET reagent. Under these conditions, **1** was treated with **2f** to afford the product (again) having a $^{31}P\{^1H\}$ NMR spectroscopic resonance at δ = 110.6 ppm ($^1J_{W,P}$ = 227.6 Hz; ca. 15%) and at δ = 105.5 ppm ($^1J_{W,P}$ = 225.1 Hz: ca. 5%) that we assign to **3f** and traces of unidentified byproducts; ca. 66% of **1** remained unreacted, which did not change significantly within 4 d. Reactions of **1** with **2g** and **2h** in the presence of $[FcH]BPh_4$ showed almost no conversion of **1** within 1 d. Nevertheless, the $^{31}P\{^1H\}$ NMR spectroscopic resonance at δ = 110.6 ppm ($^1J_{W,P}$ = 227.6 Hz) slowly increased after sev-

eral days in both reactions, and again, complex **1** did not react with **2h**.

The molecular structures of **3b** and **3d**–**e** were determined by single-crystal X-ray diffraction analysis[19] (Figures 3, 4, and 5).

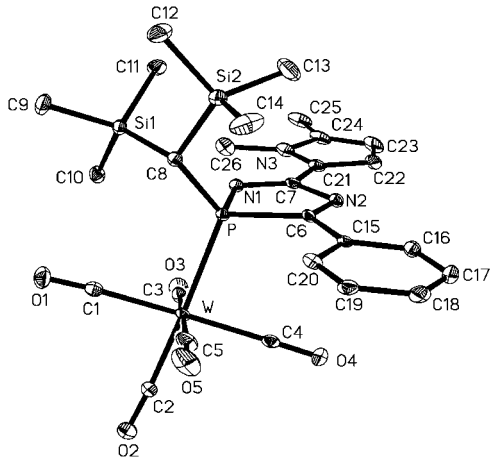

Figure 3. Molecular structure of complex **3b** in the crystal (30% probability level, hydrogen atoms are omitted for clarity). Selected bond lengths [Å] and angles [°]: W–P 2.5324(13), P–C8 1.8345(47), P–N1 1.7006(39), P–C6 1.8701(45), C6–N2 1.2947(57), N2–C7 1.4344(57), C7–N1 1.2946(59), C7–C21 1.4228(62), C6–C15 1.4876(60), N1–P–C6 89.86(19), P–C6–N2 110.00(32), C6–N2–C7 109.92(37), N2–C7–N1 119.98(40), C7–N1–P 109.80(31), P–C6–C15 127.42(33), N1–C7–C21 124.78(44).

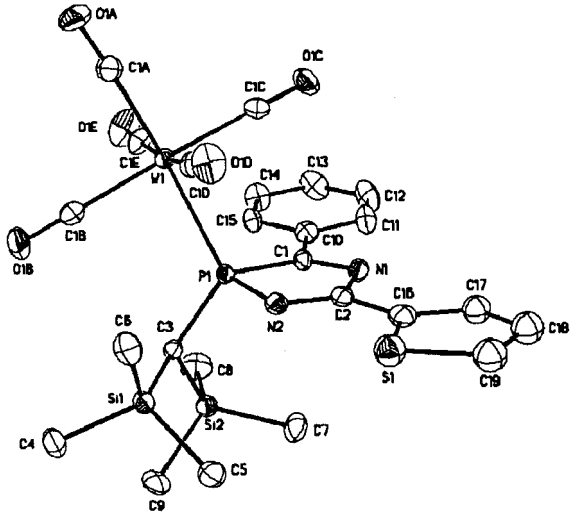

Figure 4. Molecular structure of complex **3d** in the crystal (50% probability level, hydrogen atoms and minor disordered part of the thiophene substituent are omitted for clarity). Selected bond lengths [Å] and angles [°]: W1–P1 2.531(10), P1–C3 1.835(3), P1–N2 1.707(3), P1–C1 1.877(4), C1–N1 1.304(5), N1–C2 1.424(5), C2–N2 1.293(5), C2–C16 1.441(5), C1–C10 1.457(6), N2–P1–C1 90.1(2), P1–C1–N1 109.2(3), C1–N1–C2 110.1(3), N1–C2–N2 121.0(3), C2–N2–P1 109.1(3), P1–C1–C10 129.3(3), N2–C2–C16 121.5(4).

Complexes **3b** and **3d**,**e** are isotypic. They feature almost planar phosphorus heterocycles and, to a large extent, a coplanar arrangement of the three ring systems. The torsion angles between the planes of the phosphorus heterocycle

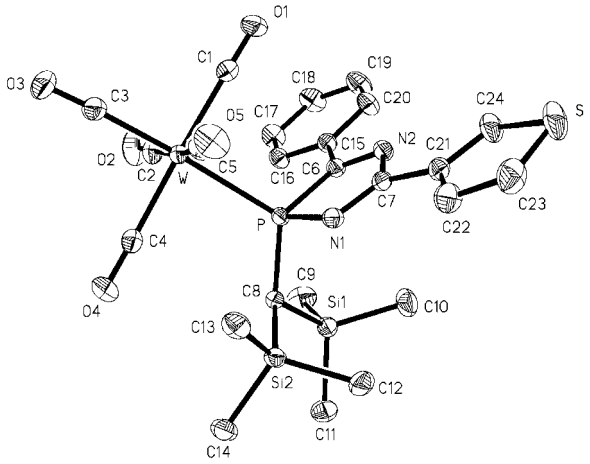

Figure 5. Molecular structure of complex **3e** in the crystal (50% probability level, hydrogen atoms are omitted for clarity). Selected bond lengths [Å] and angles [°]: W–P 2.5321(5), P–C8 1.8335(16), P–N1 1.7042(14), P–C6 1.8767(16), C6–N2 1.2990(21), N2–C7 1.4213(22), C7–N1 1.2903(21), C7–C21 1.4592(22), C6–C15 1.4675(23), N1–P–C6 90.02(7), P–C6–N2 109.14(12), C6–N2–C7 110.33(14), N2–C7–N1 120.74(14), C7–N1–P 109.31(12), P–C6–C15 128.99(12), N1–C7–C21 122.28(16).

and the particular cyclic substituent and the torsion angles between the planes of the cyclic substituents are given in Table 2. The smallest deviation from planarity is found in complex **3b**. Bond lengths and angles in the diazaphosphole ring systems of **3b** and **3d**–**e** are almost identical.

Table 2. Torsion angles of ring planes[a] for **3b** and **3d**–**e**.

	Diazaphosphole / 5-Ph	Diazaphosphole / 3-hetaryl	3-Hetaryl / 5-Ph
3b	6.68(17)	1.88(22)	5.25(20)
3d	4.29	3.47 / 9.96[b]	3.52 / 7.63[b]
3e	4.24(8)	2.79(8)	2.26(9)

[a] Torsion angles with respect to least square planes; all atoms of particular ring system involved. [b] Molecule is disordered in the crystal. Values are given for both conformations.

Theoretical Approach

The stationary points of a plausible ring-expansion pathway were calculated by DFT methods [B3LYP/TZVP//ECP-60-MWB (W)] on a model system for complex **1**, i.e. **4**. For the nitrile component, three model compounds were used, which might be classified according to their nucleophilicity: (1) medium (**2f**: R = H), (2) strong (**2i**: R = NH_2), and (3) weak (**2j**: R = CN). The influence of the solvent was taken into account by employing the COSMO approach with ε = 8.93 to mimic dichloromethane. It was shown that this approach is appropriate.[21] In consequence, computed relative free energies (Tables 3 and 4) for reactions in solution are discussed hereafter; computed stationary points are shown in Schemes 4 and 5. All relative energies, enthalpies, and free energies are available in the Supporting Information.

Table 3. Calculated thermochemical data for reactions shown in Scheme 4 (all values in kJ mol^{-1}).

Reaction		$\Delta G_{298}^{\neq}$	$\Delta_R G_{298}$
i	**4** + FcH$^+$ → **4**$^{\cdot+}$ + FcH	[a]	+139.2
ii	**4**$^{\cdot+}$ + HCN (**2f**) → **5**$^{\cdot+}$**f**	+59.8	+24.0
	4$^{\cdot+}$ + H_2NCN (**2i**) → **5**$^{\cdot+}$**i**	[b]	–13.4
iii	**4**$^{\cdot+}$ + NCCN (**2j**) → **6**$^{\cdot+}$**j** + HCN (**2f**)	+74.7	–39.5
iv	**5**$^{\cdot+}$**i** → **7**$^{\cdot+}$**i**	+22.3	–102.6
v	**5**$^{\cdot+}$**f** → **6**$^{\cdot+}$**f** + HCN (**2f**)	–1.7	–96.2
	5$^{\cdot+}$**i** → **6**$^{\cdot+}$**i** + HCN (**2f**)	+5.0	–87.5

[a] The activation barrier was not calculated. We assume an outer sphere mechanism. [b] Transition state could not be located.

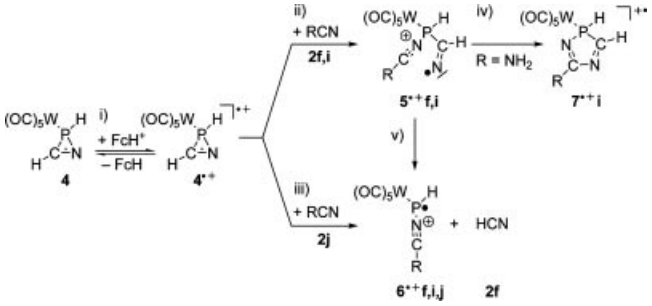

Scheme 4. Computed pathways for the reactions of 2*H*-azaphosphirene complex **4**$^{\cdot+}$ with nitrile derivatives **2f** (R = H), **2i** (R = NH_2), and **2j** (R = CN).

Table 4. Calculated thermochemical data for reactions shown in Scheme 5 (all values in kJ mol^{-1}).

Reaction		$\Delta G_{298}^{\neq}$	$\Delta_R G_{298}$
vi	**6**$^{\cdot+}$**f** + HCN (**2f**) → **7**$^{\cdot+}$**f**	+99.1	–20.5
	6$^{\cdot+}$**i** + HCN (**2f**) → **7**$^{\cdot+}$**i**	+100.6	–15.0
	6$^{\cdot+}$**j** + HCN (**2f**) → **7**$^{\cdot+}$**j**	+94.9	–52.6
vii	**6**$^{\cdot+}$**f** + HCN (**2f**) → **8**$^{\cdot+}$**f**	+116.9	–41.4
	6$^{\cdot+}$**i** + HCN (**2f**) → **8**$^{\cdot+}$**i**	+114.3	–42.6
	6$^{\cdot+}$**j** + HCN (**2f**) → **8**$^{\cdot+}$**j**	+92.9	–78.9
viii	**6**$^{\cdot+}$**f** + HCN (**2f**) → **9**$^{\cdot+}$**f**	+90.3	+75.1
	6$^{\cdot+}$**i** + HCN (**2f**) → **9**$^{\cdot+}$**i**	[a]	+108.7
	6$^{\cdot+}$**j** + HCN (**2f**) → **9**$^{\cdot+}$**j**	+77.2	+50.3
ix	**9**$^{\cdot+}$**f** → **7**$^{\cdot+}$**f**	+28.8	–95.6
	9$^{\cdot+}$**i** → **7**$^{\cdot+}$**i**	[a]	–123.7
	9$^{\cdot+}$**j** → **7**$^{\cdot+}$**j**	+32.3	–102.9
	7$^{\cdot+}$**f** + **4** → **7f** + **4**$^{\cdot+}$	[b]	–12.7
	7$^{\cdot+}$**i** + **4** → **7i** + **4**$^{\cdot+}$	[b]	–8.3
	7$^{\cdot+}$**j** + **4** → **7j** + **4**$^{\cdot+}$	[b]	–22.2

[a] Transition state could not be located. [b] The activation barrier was not calculated. We assume an outer sphere mechanism.

The overall free energy balance for net ring-expansion reactions is exergonic (cf. Schemes 4 and 5; **4** + **2f** → **7f**: $\Delta_R G_{298}$ = –104 kJ mol^{-1}, **4** + **2i** → **7i**: $\Delta_R G_{298}$ = –124 kJ mol^{-1}, and **4** + **2j** → **7j**: $\Delta_R G_{298}$ = –114 kJ mol^{-1}). Upon oxidation of **4**, 17e cationic complex **4**$^{\cdot+}$ is predicted to retain a closed-ring structure (Scheme 4); an isomer with a broken P–N bond could not be localized as an energy minimum. The oxidation by the ferrocenium cation (Scheme 4, reaction i) is predicted to be highly endergonic ($\Delta_R G_{298}$ = +139 kJ mol^{-1}), which may be due to simplification resulting from the replacement of $CH(SiMe_3)_2$ and

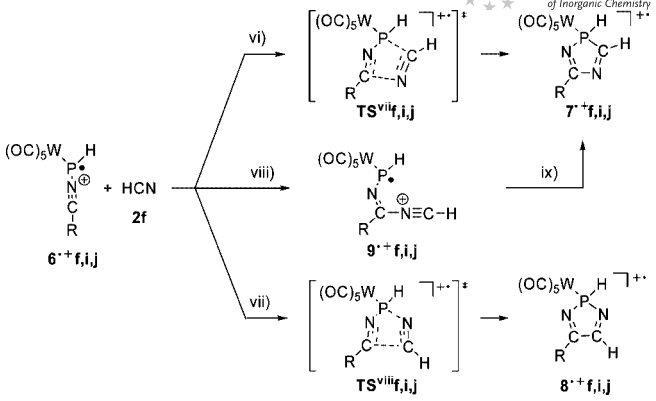

Scheme 5. Calculated pathways for the reactions of radical cationic nitrilium phosphane ylide complexes **6**$^{\cdot+}$**f,i,j** with HCN (**2f**) (**f**: R = H, **i**: R = NH_2, **j**: R = CN).

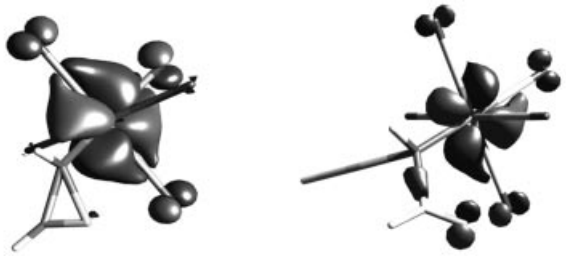

Figure 6. Highest singly occupied molecular orbitals (α-SOMO) of **4**$^{\cdot+}$ (left) and **5**$^{\cdot+}$**f** (right).

phenyl in **1** by a hydrogen atom, and thus radical cation **4**$^{\cdot+}$ is destabilized with respect to **4**. We also expect the free energy for the real system (compound **1**) to be somewhat lower but still endergonic, so the equilibrium between **1** and **1**$^{\cdot+}$ may support a low concentration of radical cation **1**$^{\cdot+}$. Most synthetically applicable radical cation chain reactions require an endergonic SET preequilibrium to initiate selective follow up reactions of highly electrophilic radical cations.[1] To save computing time we investigated the hypersurface of radical cationic model system **4**$^{\cdot+}$ by assuming that all stationary points of the reaction are affected in approximately the same way.

The highest singly occupied molecular orbital (α-SOMO) of 17e complex **4**$^{\cdot+}$, depicted in Figure 6, is mainly localized at the metal center. Only a minor participation of the nitrogen atom is apparent. An intermediate heptacoordinated tungsten complex, however, bearing one of the nitriles **2f,i,j** as ligand could not be located as an energy minimum. This ruled out a metal-centered reactivity of **4**$^{\cdot+}$ towards nitriles. Instead, a plausible pathway is the ring opening of **4**$^{\cdot+}$ by nucleophilic attack of nitriles **2f,i** with formation of intermediates **5**$^{\cdot+}$**f,i** (Scheme 4, reaction ii). The highest singly occupied molecular orbital of **5**$^{\cdot+}$**f** (Figure 6, right) also has a large contribution of the metal center, whereas a certain contribution of the nitrogen atom is apparent. This can be rationalized by the resonance structure given in Scheme 4. The barrier **TS**$^{\mathbf{ii}}$**f** for the formation of **5**$^{\cdot+}$**f** (R = H) is $\Delta G_{298}^{\neq}$ = +60 kJ mol^{-1}. For R = NH_2 no transition state

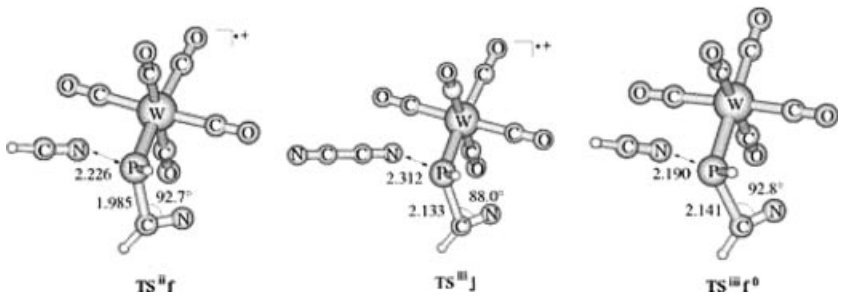

Figure 7. Transition states of the nucleophilic attack of **2f** on $\mathbf{4}^{\bullet+}$ ($\mathbf{TS}^{\mathbf{ii}}\mathbf{f}$, left), on **4** ($\mathbf{TS}^{\mathbf{iii}}\mathbf{f}^{\mathbf{0}}$, right) and of **2j** on $\mathbf{4}^{\bullet+}$ ($\mathbf{TS}^{\mathbf{iii}}\mathbf{j}$, middle).

could be located even in a constrained search, which indicates a very flat barrier. The formation of $\mathbf{5}^{\bullet+}\mathbf{f}$ is slightly endergonic ($\Delta_R G_{298}$ = +24 kJ mol^{-1}), whereas the formation of $\mathbf{5}^{\bullet+}\mathbf{i}$ is slightly exergonic ($\Delta_R G_{298}$ = –13 kJ mol^{-1}). With **2j** (R = CN), no intermediate $\mathbf{5}^{\bullet+}\mathbf{j}$ could be located. The binding of NCCN (through N) to the phosphorus center of $\mathbf{4}^{\bullet+}$ is associated with dissociation of the HCN moiety of $\mathbf{4}^{\bullet+}$ and exergonic formation of radical cationic nitrilium phosphane ylide complex $\mathbf{6}^{\bullet+}\mathbf{j}$ (Scheme 4, reaction iii; $\Delta_R G_{298}$ = –40 kJ mol^{-1}). The dissociation of HCN is indicated in transition state $\mathbf{TS}^{\mathbf{iii}}\mathbf{j}$ (Figure 7, middle) by the imaginary frequency, a 0.15 Å longer P–C distance and a 4.7° smaller P–C–N angle relative to ring-opening transition state $\mathbf{TS}^{\mathbf{ii}}\mathbf{f}$ (Figure 7, left). For the one-step substitution of HCN from $\mathbf{4}^{\bullet+}$ by nucleophilic attack of **2j**, the free activation energy $\mathbf{TS}^{\mathbf{iii}}\mathbf{j}$ was determined as $\Delta G_{298}^{\neq}$ = +75 kJ mol^{-1}. A further interesting question was to clarify the outcome of the nucleophilic attack of nitriles at the phosphorus atom of neutral 2*H*-azaphosphirene complex **4**. As indicated in the transition state, denoted as $\mathbf{TS}^{\mathbf{iii}}\mathbf{f}^{\mathbf{0}}$ (Figure 7, right), dissociation of HCN occurs also from neutral **4** upon attack of **2f**, and this reaction is also exergonic ($\Delta_R G_{298}$ = –15 kJ mol^{-1}) but the barrier is significantly higher ($\Delta G_{298}^{\neq}$ = +92 kJ mol^{-1}) than for corresponding radical cation $\mathbf{4}^{\bullet+}$. This, together with steric factors for real system **1**, might be the reason why 2*H*-azaphosphirene complex **1** does not react with nitriles in the absence of single-electron oxidants at ambient temperature.

Compound $\mathbf{5}^{\bullet+}\mathbf{i}$ (R = NH_2) can undergo cyclization to $\mathbf{7}^{\bullet+}\mathbf{i}$, a process that is predicted to be exergonic (Scheme 4, reaction iv; $\Delta_R G_{298}$ = –103 kJ mol^{-1}) and proceeding over a barrier with $\mathbf{TS}^{\mathbf{iv}}\mathbf{i}$ ($\Delta G_{298}^{\neq}$ = +22 kJ mol^{-1}). For $\mathbf{5}^{\bullet+}\mathbf{f}$ (R = H), transition state $\mathbf{TS}^{\mathbf{iv}}\mathbf{f}$ for the cyclization could not be located. A constrained decrease in the CN distance is associated with the breaking of the P–C bond. The dissociation of HCN from $\mathbf{5}^{\bullet+}\mathbf{f}$ proceeds over a very flat barrier $\mathbf{TS}^{\mathbf{v}}\mathbf{f}$ ($\Delta G_{298}^{\neq}$ = –2 kJ mol^{-1}, $\Delta E_{298}^{\neq}$ = +13 kJ mol^{-1}) yielding HCN and radical cationic nitrilium phosphane ylide complex $\mathbf{6}^{\bullet+}\mathbf{f}$ (Scheme 4, reaction v; $\Delta_R G_{298}$ = –96 kJ mol^{-1}). For $\mathbf{6}^{\bullet+}\mathbf{i}$ (R = NH_2), the HCN dissociation constitutes a competing pathway to the cyclization (Scheme 4, reaction iv). Calculated free activation energy for $\mathbf{TS}^{\mathbf{v}}\mathbf{i}$ is $\Delta G_{298}^{\neq}$ = +5 kJ mol^{-1}, and the free reaction energy is $\Delta_R G_{298}$ = –88 kJ mol^{-1}. In summary, the association of NCCN to $\mathbf{4}^{\bullet+}$ is simultaneously associated with a substitution of HCN, and on the other hand, upon the attack of HCN or H_2NCN on $\mathbf{4}^{\bullet+}$ the HCN substitution can proceed in two steps, that is, under intermediate formation of $\mathbf{5}^{\bullet+}\mathbf{f,i}$. Alternatively, for $\mathbf{5}^{\bullet+}\mathbf{i}$ (R = NH_2), cyclization to $\mathbf{7}^{\bullet+}\mathbf{i}$ is feasible.

In the highest singly occupied molecular orbital (α-SOMO) of $\mathbf{6}^{\bullet+}\mathbf{f}$ (Figure 8, left) a significant contribution of the phosphorus atom is clear (as represented by the resonance structure in Scheme 4), which is in accord with the interpretation that $\mathbf{6}^{\bullet+}\mathbf{f}$ lacks one electron of the lone pair that is assigned to phosphorus in neutral nitrilium phosphane ylide complexes.[22] In 17e cationic 2*H*-1,4,2-diazaphosphole complex $\mathbf{7}^{\bullet+}\mathbf{f}$, the α-SOMO is almost exclusively located at the metal center (Figure 8, right).

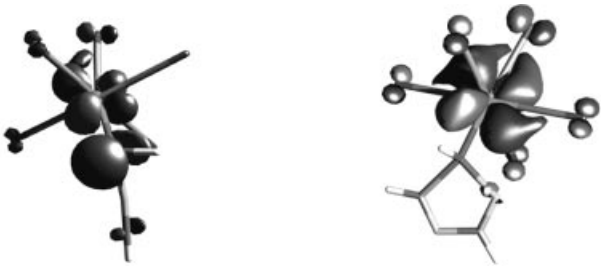

Figure 8. Highest singly occupied molecular orbitals (α-SOMO) of $\mathbf{6}^{\bullet+}\mathbf{f}$ (left) and $\mathbf{7}^{\bullet+}\mathbf{f}$ (right).

In all reactions of $\mathbf{4}^{\bullet+}$ with the three model nitrile derivatives there are plausible pathways leading to the formation of $\mathbf{6}^{\bullet+}\mathbf{f,i,j}$ with release of HCN, which in turn can (in principle) react with $\mathbf{6}^{\bullet+}\mathbf{f,i,j}$ in two regiochemically different [3+2] cycloaddition reactions, that is, with formation of radical cationic 2*H*-1,4,2-diazaphosphole complexes $\mathbf{7}^{\bullet+}\mathbf{f,i,j}$ (Scheme 5, reaction vi) or radical cationic 2*H*-1,3,2-diazaphosphole complexes $\mathbf{8}^{\bullet+}\mathbf{f,i,j}$ (Scheme 5, reaction vii). All reactions are exergonic (Table 4) and 2*H*-1,3,2-diazaphosphole complexes $\mathbf{8}^{\bullet+}\mathbf{f,i,j}$ are ca. 20–30 kJ mol^{-1} more stable than corresponding 2*H*-1,4,2-diazaphosphole complexes $\mathbf{7}^{\bullet+}\mathbf{f,i,j}$. For the reactions of $\mathbf{6}^{\bullet+}\mathbf{f,i}$ (R = H and R = NH_2) with HCN the barriers $\mathbf{TS}^{\mathbf{vi}}\mathbf{f,i}$ for the formation of $\mathbf{7}^{\bullet+}\mathbf{f,i}$ are 18 and 14 kJ mol^{-1} lower than those for the formation of $\mathbf{8}^{\bullet+}\mathbf{f,i}$ ($\mathbf{TS}^{\mathbf{vii}}\mathbf{f,i}$). For the reactions of $\mathbf{6}^{\bullet+}\mathbf{j}$ (R = CN) with HCN the barriers $\mathbf{TS}^{\mathbf{vi}}\mathbf{j}$ and $\mathbf{TS}^{\mathbf{vii}}\mathbf{j}$ are approximately equal.

For the reaction of $\mathbf{6}^{\bullet+}\mathbf{f,i,j}$ with HCN a further alternative pathway is plausible, namely a stepwise mechanism starting with the addition of HCN to $\mathbf{6}^{\bullet+}\mathbf{f,i,j}$, which leads to the

formation of a C–N bond to yield intermediates **9**$^{\cdot+}$**f**,**i**,**j** (Scheme 5, reaction viii), with subsequent cyclization to **7**$^{\cdot+}$**f**,**i**,**j** (Scheme 5, reaction ix). The barriers for C–N bond formation **TS**$^{\mathbf{viii}}$**f**,**j** ($\Delta G_{298}^{\neq}$ = +90 kJ mol^{-1} for the reaction of HCN with **6**$^{\cdot+}$**f** and $\Delta G_{298}^{\neq}$ = +77 kJ mol^{-1} for the reaction with **6**$^{\cdot+}$**j**) are slightly lower than those for the corresponding direct [3+2] cycloaddition **TS**$^{\mathbf{vi}}$**f**,**j**, whereas the barriers for the second step **TS**$^{\mathbf{ix}}$**f**,**j** are almost negligible ($\Delta G_{298}^{\neq}$ = +29 kJ mol^{-1} for **9**$^{\cdot+}$**f** and $\Delta G_{298}^{\neq}$ = +32 kJ mol^{-1} for **9**$^{\cdot+}$**j**). The formation of **9**$^{\cdot+}$**f**,**i**,**j** (Scheme 5, reaction viii) is predicted to be endergonic for our three model reactions, that is, for the reaction of HCN with **6**$^{\cdot+}$**f** $\Delta_R G_{298}$ = +75 kJ mol^{-1}, for the reaction with **6**$^{\cdot+}$**j** $\Delta_R G_{298}$ = +50 kJ mol^{-1}, and especially for the reaction with **6**$^{\cdot+}$**i** $\Delta_R G_{298}$ = +109 kJ mol^{-1}.

Once **7**$^{\cdot+}$**f**,**i**,**j** are formed, the cycle is closed by the oxidation of 2*H*-azaphosphirene complex **4** by **7**$^{\cdot+}$**f**,**i**,**j** (for **7**$^{\cdot+}$**f**: $\Delta_R G_{298}$ = –13 kJ mol^{-1}, for **7**$^{\cdot+}$**i**: $\Delta_R G_{298}$ = –8 kJ mol^{-1}, for **7**$^{\cdot+}$**j**: $\Delta_R G_{298}$ = –22 kJ mol^{-1}) to yield 2*H*-1,4,2-diazaphosphole complexes **7f**,**i**,**j** and **4**$^{\cdot+}$, which then can restart the chain reaction (Scheme 3).

Conclusions

A combined experimental and theoretical investigation on the ring expansion of 2*H*-azaphosphirene complex **1** with a wide variety of electronically different nitriles revealed that electron-rich nitrile derivatives **2a**–**e** furnish regioselectively 2*H*-1,4,2-diazaphosphole complexes **3a**–**e** in the presence of substoichiometric amounts of ferrocenium hexafluorophosphate. The reaction course shows characteristics of an autocatalytic reaction and is interpretable in terms of a ligand-centered reactivity of an organometallic radical cation (**1**$^{\cdot+}$). In contrast, reactions of complex **1** with **2f**–**h** proceeded differently. With HCN (**2f**) complex **3f** was formed slowly and not selectively; byproducts having a P–F bond were also formed. This provides the first strong evidence that transiently formed highly electrophilic phosphorus-containing species had reacted with hexafluorophosphate through fluoride transfer. In reactions of complex **1** with weak nucleophilic nitrile derivatives **2g**,**h**, byproducts bearing a P–F bond were also formed, but the formation of 2*H*-1,4,2-diazaphosphole complexes **3g**,**h** could not be detected.

The computational results can be summarized as follows: The barrier of the nucleophilic attack of the nitrile at radical cationic complex **4**$^{\cdot+}$ depends strongly on its nucleophilicity. As a result of steric factors in the real system of **1**, this step may be crucial. The further course of the ring expansion with strong nucleophilic nitrile derivatives[23] can proceed by direct cyclization of the intermediately formed complex **5**$^{\cdot+}$ or with moderately nucleophilic nitrile derivatives by formation of complex **6**$^{\cdot+}$ accompanied by the release of nitrile and subsequent [3+2] cycloaddition. Because the reactions are performed at ambient temperature, the kinetically controlled pathway proceeding via the more favorable transition state may be preferred, which yields regioselectively 2*H*-1,4,2-diazaphosphole complexes **7**$^{\cdot+}$. As experimentally shown, complex **1** reacts with weak nucleophilic nitrile derivatives **2g**,**h** in the presence of ferrocenium salts neither to 2*H*-1,4,2-diazaphosphole complexes **3g**,**h** nor to 2*H*-1,3,2-diazaphosphole complexes **8g**,**h**. If hexafluorophosphate is present, products bearing a P–F bond are formed. So, in the presence of weak nucleophilic nitrile derivatives a completely different reaction course is taken, which proceeds with the participation of the hexafluorophosphate anion.

Experimental Section

General Procedures: All reactions and manipulations were carried out under an atmosphere of deoxygenated, dried nitrogen or argon by using standard Schlenk techniques with conventional glassware. Solvents were dried according to standard procedures. 2*H*-Azaphosphirene complex **1** was synthesized according to the method described in the literature.[10d] NMR spectra were recorded with a Bruker AC-200 spectrometer or a Bruker Avance 300 spectrometer with [D$_6$]benzene or [D]chloroform as solvent and internal standard; shifts are given relative to external tetramethylsilane (^{1}H, ^{13}C), neat $CFCl_3$ (^{19}F), and 85% H_3PO_4 (^{31}P). Mass spectra were recorded with a Finnigan MAT 8430 (70 eV) or a Kratos Concept 1H spectrometer (FAB+, *m*NBA); apart from *m*/*z* values of the molecule ions, only *m*/*z* values having intensities more than 10% are given. Infrared spectra were recorded with a Biorad FTIR 165 (selected data given) or a Bruker FTIR IFS113V spectrometer. UV/Vis spectra were recorded with a Shimadzu UV-1650 PC spectrometer. Melting points were obtained with a Büchi 535 capillary apparatus or a Büchi apparatus Type S. The values are not corrected. Elemental analyses were performed using a Carlo Erba analytical gas chromatograph or an Elementar VarioEL instrument.

General Procedure for the Synthesis of 3a–e: To a solution of 2*H*-azaphosphirene complex **1** (617 mg, 1.00 mmol) in CH_2Cl_2 (3 mL) was added the appropriate nitrile (**2a**: 122 μL, 1.50 mmol; **2b**: 120 mg, 1.00 mmol; **2c**: 180 μL, 2.06 mmol; **2d**: 94 μL, 1.01 mmol; **2e**: 94 μL, 1.03 mmol) and ferrocenium hexafluorophosphate (17 mg, 0.05 mmol). The reaction mixture was stirred for 6 h at ambient temperature [reaction monitoring by ^{31}P{^{1}H} NMR spectroscopy]. After the solvent was removed in vacuo, the product was separated and purified by column chromatography (SiO_2, –10 °C, petroleum ether ether/Et_2O, 97.5:2.5).

Complex 3a: Yield: 406 mg (0.59 mmol, 59%). Yellow solid, recrystallized from *n*-pentane. M.p. 122 °C. ^{1}H NMR (300.13 MHz, C_6D_6, 30 °C): δ = –0.22 (s, 9 H, $SiMe_3$), 0.50 (s, 9 H, $SiMe_3$), 1.01 [d, $^2J_{P,H}$ = 5.8 Hz, 1 H, C*H*($SiMe_3$)$_2$], 2.78 (s, 3 H, NMe), 2.92 (s, 3 H, NMe), 7.11 (m$_c$, 3 H, *meta*, *para* Ph), 8.17 (m$_c$, 2 H, *ortho* Ph) ppm. ^{13}C{^{1}H} NMR (75.5 MHz, C_6D_6, 30 °C): δ = 3.1 [d, $^3J_{P,C}$ = 1.6 Hz, Si(CH_3)$_3$], 4.1 [d, $^3J_{P,C}$ = 2.6 Hz, Si(CH_3)$_3$], 22.0 [d, $^1J_{P,C}$ = 5.8 Hz, *C*H($SiMe_3$)$_2$], 37.6 (s, NCH_3), 37.6 (s, NCH_3), 128.8 (s, *para* Ph), 131.6 (d, $^3J_{P,C}$ = 1.9 Hz, *ortho* Ph), 132.8 (d, $^2J_{P,C}$ = 20.7 Hz, *ipso* Ph), 133.3 (s, *meta* Ph), 165.0 (s, PNC), 198.6 (d$_{sat}$, $^2J_{P,C}$ = 6.5 Hz, $^1J_{W,C}$ = 126.7 Hz, *cis* CO), 199.6 (d, $^2J_{P,C}$ = 22.3 Hz, *trans* CO), 200.3 (d, $^{[1+4]}J_{P,C}$ = 25.5 Hz, PCN) ppm. ^{31}P{^{1}H} NMR (121.5 MHz, C_6D_6, 30 °C): δ = 101.8 (s$_{sat}$, $^1J_{W,P}$ = 241.6 Hz) ppm. IR (KBr): $\tilde{\nu}$ = 2068 (CO), 1980 (CO), 1922 (CO) cm^{-1}. MS (FAB+, *m*NBA): *m*/*z* (%) = 688.1 (12) [M + H]$^+$, 659.1 (49) [M – CO]$^+$, 631.1 (38) [M – 2 CO]$^+$, 603.1 (10) [M – 3 CO]$^+$, 364.2 (100) [M – W(CO)$_5$ + H]$^+$. $C_{22}H_{30}N_3O_5PSi_2W$ (687.48): calcd. C 38.44, H 4.40, N 6.11; found C 38.49, H 4.54, N 5.86.

Complex 3b: Yield: 398 mg (0.54 mmol, 54%). Orange solid, recrystallized from *n*-pentane. M.p. 123 °C. ^{1}H NMR (200 MHz, $CDCl_3$, 25 °C): δ = –0.10 (s, 9 H, $SiMe_3$), 0.52 (s, 9 H, $SiMe_3$), 1.19 (d, $^2J_{P,H}$ = 3.9 Hz, 1 H, C*H*$SiMe_3$), 2.37 (s, 3 H, CMe), 4.08 (s, 3 H, NMe), 6.11 (d, $^3J_{H,H}$ = 3.9 Hz, 1 H, 3-pyrryl), 7.52 (m_c, 5 H, *meta*, *para* Ph, 4-pyrryl), 8.23 (dd, $^4J_{H,H}$ = 2.2 Hz, $^3J_{H,H}$ = 7.6 Hz, 2 H, *ortho* Ph) ppm. ^{13}C{^{1}H} NMR (50.3 MHz, $CDCl_3$, 25 °C): δ = 2.9 [d, $^3J_{P,C}$ = 2.0 Hz, $Si(CH_3)_3$], 3.7 [d, $^3J_{P,C}$ = 2.7 Hz, $Si(CH_3)_3$], 13.0 (s, CMe), 19.8 [d, $^1J_{P,C}$ = 5.4 Hz, *C*H$(SiMe_3)_2$], 109.0 (s, 4-pyrryl), 122.4 (s, 3-pyrryl), 127.6 (d, $^2J_{P,C}$ = 12.1 Hz, 2-pyrryl), 128.7 (s, *meta* Ph), 131.2 (d, $^3J_{P,C}$ = 2.0 Hz, *ortho* Ph), 132.4 (d, $^2J_{P,C}$ = 23.5 Hz, *ipso* Ph), 132.9 (s, *para* Ph), 139.7 (s, 5-pyrryl), 162.3 (d, $^{[2+3]}J_{P,C}$ = 5.8 Hz, PNC), 197.5 (d, $^2J_{P,C}$ = 6.4 Hz, *cis* CO), 197.0 (d, $^{[1+4]}J_{P,C}$ = 22.7 Hz, PCN), 198.8 (d, $^2J_{P,C}$ = 13.5 Hz, *trans* CO) ppm. ^{31}P{^{1}H} NMR (81.0 MHz, $CDCl_3$, 25 °C): δ = 108.4 (s_{sat}, $^1J_{W,P}$ = 233.9 Hz) ppm. IR (KBr): $\tilde{\nu}$ = 2071 (CO), 1994 (CO), 1926 (CO), 1873 (CO) cm^{-1}. MS (EI, 70 eV, ^{184}W): *m/z* (%) = 726 (8) $[M]^+$, 698 (16) $[M – CO]^+$, 670 (32) $[M – 2\ CO]^+$, 533 (52) [M – 3 CO – $C_7H_9N_2]^+$, 73 (100) $[SiMe_3]^+$. $C_{26}H_{32}N_3O_5PSi_2W$ (737.53): calcd. C 42.22, H 4.51, N 5.48; found C 42.29, H 4.50, N 5.51.

Complex 3c: Yield: 404 mg (0.57 mmol, 57%). Orange solid, recrystallized from *n*-pentane. M.p. 119 °C. ^{1}H NMR (200 MHz, $CDCl_3$, 25 °C): δ = –0.10 (s, 9 H, $SiMe_3$), 0.54 (s, 9 H, $SiMe_3$), 1.16 (d, 1 H, $^2J_{P,H}$ = 4.1 Hz, 1 H, C*H*$SiMe_3$), 6.64 (dd, $^3J_{H,H}$ = 3.5 Hz, $^3J_{H,H}$ = 1.8 Hz, 2 H, 4-furanyl), 7.56 (m_c, 4 H, *meta*, *para* Ph, 4-furanyl), 7.72 (m_c, $^3J_{H,H}$ = 1.8 Hz, 1 H, 5-furanyl), 8.21 (dd, 2 H, $^4J_{H,H}$ = 2.7 Hz, $^3J_{H,H}$ = 5.9 Hz, 2 H, *ortho* Ph) ppm. ^{13}C{^{1}H} NMR (50.3 MHz, $CDCl_3$, 25 °C): δ = 2.9 [d, $^3J_{P,C}$ = 2.0 Hz, $Si(CH_3)_3$], 3.7 [d, $^3J_{P,C}$ = 2.8 Hz, $Si(CH_3)_3$], 18.8 [d, $^1J_{P,C}$ = 5.2 Hz, *C*H-$(SiMe_3)_2$], 112.5 (s, 4-furanyl), 119.6 (s, 3-furanyl), 128.9 (s, *meta* Ph), 131.3 (d, $^3J_{P,C}$ = 2.1 Hz, *ortho* Ph), 132.2 (d, $^2J_{P,C}$ = 22.7 Hz, *ipso* Ph), 133.6 (s, *para* Ph), 147.4 (s, 5-furanyl), 149.3 (d, $^3J_{P,C}$ = 14.5 Hz, 2-furanyl), 160.2 (d, $^{[2+3]}J_{P,C}$ = 3.8 Hz, PNC), 197.1 (d, $^2J_{P,C}$ = 6.1 Hz, *cis* CO), 198.2 (d, $^{[1+4]}J_{P,C}$ = 22.4 Hz, PCN), 202.1 (d, $^2J_{P,C}$ = 22.7 Hz, *trans* CO) ppm. ^{31}P{^{1}H} NMR (81.0 MHz, $CDCl_3$, 25 °C): δ = 110.6 (s_{sat}, $^1J_{W,P}$ = 230.6 Hz). MS (EI, 70 eV, ^{184}W): *m/z* (%) = 710 (11) $[M]^+$, 682 (11) $[M – CO]^+$, 654 (85) $[M – 3\ CO]^+$, 533 (52) [M – 3 CO – $C_5H_3NO]^+$, 477 (52) [M – 5 CO – $C_5H_3NO]^+$, 73 (100) $[SiMe_3]^+$. $C_{24}H_{27}N_2O_6PSi_2W$ (710.47): calcd. C 40.57, H 3.83, N 3.94; found C 40.72, H 3.83, N 3.94.

Complex 3d: Yield: 371 mg (0.51 mmol, 51%). Orange solid, recrystallized from *n*-pentane. M.p. 112 °C. ^{1}H NMR (200 MHz, $CDCl_3$, 25 °C): δ = –0.09 (s, 9 H, $SiMe_3$), 0.53 (s, 9 H, $SiMe_3$), 1.19 [d, $^2J_{P,H}$ = 4.0 Hz, 1 H, $CH(SiMe_3)_2$], 7.24 (m_c, 1 H, 3-thienyl), 7.57 (m_c, 4 H, *meta*, *para* Ph, 4-thienyl), 8.22 (m_c, 1 H, 2-thienyl), 8.24 (dd, $^4J_{H,H}$ = 1.7 Hz, $^3J_{H,H}$ = 7.5 Hz, 2 H, *ortho* Ph) ppm. ^{13}C{^{1}H} NMR (50.3 MHz, C_6D_6, 25 °C): δ = 2.9 [d, $^3J_{P,C}$ = 2.1 Hz, $Si(CH_3)_3$], 3.7 [d, $^3J_{P,C}$ = 2.6 Hz, $Si(CH_3)_3$], 18.9 [d, $^1J_{P,C}$ = 5.0 Hz, *C*H$(SiMe_3)_2$], 128.5 (s, 4-thienyl), 128.9 (s, *meta* Ph), 131.4 (d, $^3J_{P,C}$ = 2.1 Hz, *ortho* Ph), 132.3 (d, $^2J_{P,C}$ = 22.5 Hz, *ipso* Ph), 133.1 (s, 5-thienyl), 133.6 (s, *para* Ph), 134.0 (s, 3-thienyl), 138.5 (d, $^3J_{P,C}$ = 14.4 Hz, *2*-thienyl), 164.4 (d, $^{[2+3]}J_{P,C}$ = 4.0 Hz, PNC), 197.1 (d, $^2J_{P,C}$ = 6.3 Hz, *cis* CO), 198.2 (d, $^2J_{P,C}$ = 22.4 Hz, *trans* CO), 201.3 (d, $^{[1+4]}J_{P,C}$ = 23.2 Hz, PCN) ppm. ^{31}P{^{1}H} NMR (81.0 MHz, C_6D_6, 25 °C): δ = 110.5 (s_{sat}, $^1J_{W,P}$ = 229.5 Hz) ppm. IR (KBr): $\tilde{\nu}$ = 2952 (CH), 2899 (CH), 2073 (CO), 2001 (CO), 1909 (CO), 1413 (thienyl), 1253 (thienyl) cm^{-1}. MS (EI, 70 eV, ^{184}W): *m/z* (%) = 726 (8) $[M]^+$, 698 (16) $[M – CO]^+$, 670 (32) $[M – 2\ CO]^+$, 73 (100) $[SiMe_3]^+$. $C_{24}H_{27}N_2O_5PSSi_2W$ (726.53): calcd. C 39.68, H 3.75, N 3.86, S 4.41; found C 39.82, H 3.70, N 4.64, S 3.79.

Complex 3e: Yield: 378 mg (0.52 mmol, 52%). Orange solid, recrystallized from *n*-pentane. M.p. 112 °C. ^{1}H NMR (200 MHz, $CDCl_3$, 25 °C): δ = 0.00 (s, 9 H, $SiMe_3$), 0.64 (s, 9 H, $SiMe_3$), 1.30 (d, $^2J_{P,H}$ = 4.1 Hz, 1 H, C*H*$SiMe_3$), 6.87 (m_c, 1 H, 4-thienyl), 7.65 (m_c, 3 H, *meta*, *para* Ph), 7.99 (d, $^3J_{H,H}$ = 4.9 Hz, 1 H, 5-thienyl), 8.34 (d, $^3J_{H,H}$ = 6.8 Hz, 2 H, *ortho* Ph) ppm. ^{13}C{^{1}H} NMR (50.3 MHz, 25 °C, $CDCl_3$): δ = 2.9 [d, $^3J_{P,C}$ = 1.9 Hz, $Si(CH_3)_3$], 3.7 [d, $^3J_{P,C}$ = 2.6 Hz, $Si(CH_3)_3$], 18.6 [d, $^1J_{P,C}$ = 4.8 Hz, *C*H$(SiMe_3)_2$], 126.6 (s, 2-thienyl), 128.1 (s, 5-thienyl), 128.6 (s, *meta* Ph), 131.2 (d, $^3J_{P,C}$ = 2.1 Hz, *ortho* Ph), 132.6 (d, $^2J_{P,C}$ = 23.8 Hz, *ipso* Ph), 133.4 (s, *para* Ph), 133.6 (s, 4-thienyl), 137.2 (d, $^3J_{P,C}$ = 13.6 Hz, 3-thienyl), 165.0 (d, $^{[2+3]}J_{P,C}$ = 4.9 Hz, PNC), 197.1 (d, $^2J_{P,C}$ = 5.9 Hz, *cis* CO), 198.2 (d, $^{[1+4]}J_{P,C}$ = 22.4 Hz, PCN), 201.8 (d, $^2J_{P,C}$ = 22.8 Hz, *trans* CO) ppm. ^{31}P{^{1}H} NMR (81.0 MHz, $CDCl_3$, 25 °C): δ = 109.1 (s_{sat}, $^1J_{W,P}$ = 229.8 Hz). IR (KBr): $\tilde{\nu}$ = 2073 (s, CO), 2000 (s, CO), 1921 (s, sh, CO), 1253 (m, thienyl), 834 (w, thienyl) cm^{-1}. MS (EI, 70 eV, ^{184}W): *m/z* (%) = 726 (12) $[M]^+$, 698 (26) $[M – CO]^+$, 670 (100) $[M – 2\ CO]^+$, 533 (26) [M – 3 CO – $C_5H_3NS]^+$, 477 (38) [M – 5 CO – $C_5H_3NS]^+$, 73 (74) $[SiMe_3]^+$. $C_{24}H_{27}N_2O_5PSSi_2W$ (726.53): calcd. C 39.69, H 3.75, N 3.86, S 4.41; found C 39.34, H 3.98, N 3.46, S 4.36.

Investigation of the Dependence of the Reaction Progression of 1 with 2d on the Amount of Ferrocenium Hexafluorophosphate: To a solution of 2*H*-azaphosphirene complex **1** (123 mg, 0.20 mmol) in CH_2Cl_2 (0.6 mL) was added 2-thiophene carbonitrile **2d** (19 μL, 0.20 mmol) and the appropriate amount of ferrocenium hexafluorophosphate (0.7 mg, 0.002 mmol; 1.3 mg, 0.004 mmol; 2.0 mg, 0.006 mmol; 2.6 mg, 0.008 mmol; 3.3 mg, 0.010 mmol; 6.6 mg, 0.020 mmol; 9.9 mg, 0.030 mmol; 13.2 mg, 0.040 mmol). Product ratios were estimated by ^{31}P{^{1}H} NMR spectroscopic resonance integration (30 °C, 100 scans each, measurement duration 159 s, recorded reaction time corresponds to the end of the respective measurement). For the investigations corresponding to Figure 2, a solution of $[FcH]PF_6$ (1.6 mg, 0.005 mmol) and 2-thiophene carbonitrile **2d** (19 μL, 0.20 mmol) in CH_2Cl_2 was added to 2*H*-azaphosphirene complex **1** (123 mg, 0.20 mmol) to ensure that the entire amount of $[FcH]PF_6$ was diluted at the start of the reaction. Product ratios were estimated by ^{31}P{^{1}H} NMR spectroscopic resonance integration (30 °C, 32 scans each, measurement duration 56 s).

Attempted Synthesis of Complex 3f with the Use of Ferrocenium Hexafluorophosphate: To a solution of 2*H*-azaphosphirene complex **1** (123 mg, 0.20 mmol) in CH_2Cl_2 (0.6 mL) was added hydrogen cyanide **2f** (20 μL, 0.51 mmol) and ferrocenium hexafluorophosphate (12 mg, 0.04 mmol). The reaction mixture was stirred at ambient temperature [reaction monitored by ^{31}P{^{1}H} NMR spectroscopy]. After 4 d the reaction mixture containing unidentified products **A**–**F** and **3f** was analyzed by ^{31}P{^{1}H} NMR and ^{19}F{^{1}H} NMR spectroscopy at 30 °C [ratio estimation by ^{31}P{^{1}H} NMR resonance integration]. ^{31}P{^{1}H} NMR (121.5 MHz, CH_2Cl_2): δ = 206.9 [d, $^1J_{P,F}$ = 855.8 Hz, **A** (1%)], 206.2 [d, $^1J_{P,F}$ = 841.8 Hz, **B** (3%)], 197.3 [d, $^1J_{P,F}$ = 824.0 Hz, **C** (9%)], 191.2 [d, $^1J_{P,F}$ = 989.3 Hz, **D** (4%)], 161.2 [s_{sat}, $^1J_{W,P}$ = 289.9 Hz, **E** (6%)], 110.7 [s_{sat}, $^1J_{W,P}$ = 227.6 Hz, **F** (5%)], 105.5 [s_{sat}, $^1J_{W,P}$ = 225.1 Hz, **3f** (20%)], –109.9 [s_{sat}, $^1J_{W,P}$ = 293.7 Hz, **1** (16%)], –143.5 [sept, $^1J_{P,F}$ = 714.0 Hz, PF_6^- (3%)] ppm. ^{19}F{^{1}H} NMR (282.4 MHz, CH_2Cl_2): δ = –31.0 [d, $^1J_{P,F}$ = 991.8 Hz, **D** (4%)], –72.5 [d, $^1J_{P,F}$ = 713.6 Hz, PF_6^- (3%)], –109.1 [d, $^1J_{P,F}$ = 841.5 Hz, **B** (3%)], –111.4 [d, $^1J_{P,F}$ = 854.9 Hz, **A** (1%)], –117.2 [d, $^1J_{P,F}$ = 823.5 Hz, **C** (9%)] ppm.

Attempted Synthesis of Complex 3g with the Use of Ferrocenium Hexafluorophosphate: To a solution of 2*H*-azaphosphirene complex **1** (123 mg, 0.20 mmol) in CH_2Cl_2 (0.6 mL) was added ethyl cyanoformate **2g** (30 μL, 0.30 mmol) and ferrocenium hexafluorophos-

phate (12 mg, 0.04 mmol). The reaction mixture was stirred at ambient temperature [reaction monitored by $^{31}P\{^1H\}$ NMR spectroscopy]. After 6 d, the reaction mixture was analyzed by $^{31}P\{^1H\}$ NMR and $^{19}F\{^1H\}$ NMR spectroscopy at 30 °C [ratio estimation by $^{31}P\{^1H\}$ NMR resonance integration]. $^{31}P\{^1H\}$ NMR (121.5 MHz, CH_2Cl_2): δ = 197.3 [d, $^1J_{P,F}$ = 822.7 Hz, **A** (12%)], 177.2 [d, $^1J_{P,F}$ = 967.7 Hz, **B** (2%)], 160.8 [s_{sat}, $^1J_{W,P}$ = 284.8 Hz, **C** (6%)], 110.7 [s_{sat}, $^1J_{W,P}$ = 227.6 Hz, **D** (21%)], 18.5 [d, $^1J_{P,F}$ = 1044.0 Hz, **E** (3%)], –110.1 [s_{sat}, $^1J_{W,P}$ = 293.7 Hz, **1** (41%)], –143.8 [sept, $^1J_{P,F}$ = 714.0 Hz, PF_6^- (6%)] ppm. $^{19}F\{^1H\}$ NMR (282.4 MHz, CH_2Cl_2): δ = –66.7 [d, $^1J_{P,F}$ = 1046.8 Hz, **E** (3%)], –73.8 [d, $^1J_{P,F}$ = 712.5 Hz, PF_6^- (6%)], –74.4 [d, $^1J_{P,F}$ = 968.3 Hz, **B** (2%)], –117.2 [d, $^1J_{P,F}$ = 823.5 Hz, **A** (12%)] ppm.

Attempted Synthesis of Complex 3h with the Use of Ferrocenium Hexafluorophosphate: To a solution of 2*H*-azaphosphirene complex **1** (123 mg, 0.20 mmol) in CH_2Cl_2 (0.6 mL) was added 2,3,4,5,6-pentafluorobenzonitrile **2h** (160 μL, 1.27 mmol) and ferrocenium hexafluorophosphate (12 mg, 0.04 mmol). The reaction mixture was stirred at ambient temperature [reaction monitored by $^{31}P\{^1H\}$ NMR spectroscopy]. After 6 d the reaction mixture containing unidentified products **A**–**F**, **1**, and **2h** was analyzed by $^{31}P\{^1H\}$ NMR and $^{19}F\{^1H\}$ NMR spectroscopy at 30 °C [ratio estimation by $^{31}P\{^1H\}$ NMR resonance integration]. $^{31}P\{^1H\}$ NMR (121.5 MHz, CH_2Cl_2): δ = 197.4 [d, $^1J_{P,F}$ = 824.0 Hz, $^1J_{W,P}$ = 286.1 Hz, **A** (11%)], 183.1 [s, **B** (5%)], 176.3 [s, **C** (5%)], 160.9 [s_{sat}, $^1J_{W,P}$ = 282.3 Hz, **D** (5%)], 110.7 [s_{sat}, $^1J_{W,P}$ = 228.9 Hz, **E** (12%)], 18.4 [d, $^1J_{P,F}$ = 1041.4 Hz, **F** (3%)], –110.4 [s_{sat}, $^1J_{W,P}$ = 293.7 Hz, **1** (48%)] ppm. $^{19}F\{^1H\}$ NMR (282.4 MHz, CH_2Cl_2): δ = –67.6 [d, $^1J_{P,F}$ = 1041.2 Hz, **F** (3%)], –75.5 (d, $^1J_{P,F}$ = 713.6 Hz, PF_6^-), –117.6 [d, $^1J_{P,F}$ = 823.5 Hz, **A** (11%)], –134.0 (m_c, **2h**), –144.7 (m_c, **2h**), –160.6 (m_c, **2h**) ppm.

Synthesis of 3d with the Use of Ferrocenium Tetraphenylborate: To a solution of 2*H*-azaphosphirene complex **1** (62 mg, 0.10 mmol) in CH_2Cl_2 (0.3 mL) was added 2-thiophene carbonitrile **2d** (10 μL, 0.11 mmol) and ferrocenium tetraphenylborate (9 mg, 0.02 mmol). The reaction mixture was stirred for 8 h at ambient temperature, and the complete formation of **3d** was evidenced by analysis of the reaction mixture by $^{31}P\{^1H\}$ NMR spectroscopy.

Attempted Synthesis of Complex 3f with the Use of Ferrocenium Tetraphenylborate: To a solution of 2*H*-azaphosphirene complex **1** (123 mg, 0.20 mmol) in CH_2Cl_2 (0.6 mL) was added hydrogen cyanide **2f** (20 μL, 0.51 mmol) and ferrocenium tetraphenylborate (18 mg, 0.04 mmol). The reaction mixture was stirred at ambient temperature [reaction monitored by $^{31}P\{^1H\}$ NMR spectroscopy]. After 4 d the reaction mixture containing unidentified products **A**–**D** and **1** was analyzed by $^{31}P\{^1H\}$ NMR spectroscopy at 30 °C [ratio estimation by $^{31}P\{^1H\}$ NMR resonance integration]. $^{31}P\{^1H\}$ NMR (121.5 MHz, CH_2Cl_2): δ = 110.6 [s_{sat}, $^1J_{W,P}$ = 227.6 Hz, **A** (13%)], 105.5 [s_{sat}, $^1J_{W,P}$ = 223.8 Hz, **3f** (3%)], 20.7 [s_{sat}, $^1J_{W,P}$ = 236.5 Hz, **B** (3%)], 13.2 [s_{sat}, $^1J_{W,P}$ = 236.5 Hz, **C** (8%)], –68.9 [s_{sat}, $^1J_{W,P}$ = 242.9 Hz, **D** (17%)], –109.9 [s_{sat}, $^1J_{W,P}$ = 293.7 Hz, **1** (37%)] ppm.

Attempted Synthesis of Complex 3g with the Use of Ferrocenium Tetraphenylborate: To a solution of 2*H*-azaphosphirene complex **1** (123 mg, 0.20 mmol) in CH_2Cl_2 (0.6 mL) was added ethyl cyanoformate **2g** (30 μL, 0.30 mmol) and ferrocenium tetraphenylborate (18 mg, 0.04 mmol). The reaction mixture was stirred at ambient temperature [reaction monitored by $^{31}P\{^1H\}$ NMR spectroscopy]. After 6 d the reaction mixture containing unidentified products **A**–**G** and **1** was analyzed by $^{31}P\{^1H\}$ NMR spectroscopy at 30 °C [ratio estimation by $^{31}P\{^1H\}$ NMR resonance integration]. $^{31}P\{^1H\}$ NMR (121.5 MHz, CH_2Cl_2): δ = 204.9 [**A** (1%)], 184.5 [**B** (1%)], 163.3 [**C** (1%)], 110.7 [**D** (1%)], 97.4 [**E** (1%)], 54.5 [**F** (1%)], 34.1 [**G** (10%)], –110.1 [s_{sat}, $^1J_{W,P}$ = 293.7 Hz, **1** (81%)] ppm.

Attempted Synthesis of Complex 3h with the Use of Ferrocenium Tetraphenylborate: To a solution of 2*H*-azaphosphirene complex **1** (123 mg, 0.20 mmol) in CH_2Cl_2 (0.6 mL) was added 2,3,4,5,6-pentafluorobenzonitrile **2h** (160 μL, 1.27 mmol) and ferrocenium hexafluorophosphate (18 mg, 0.04 mmol). The reaction mixture was stirred at ambient temperature [reaction monitored by $^{31}P\{^1H\}$ NMR spectroscopy]. After 6 d the reaction mixture containing unidentified products **A**–**H** and **2h** was analyzed by $^{31}P\{^1H\}$ NMR and $^{19}F\{^1H\}$ NMR spectroscopy at 30 °C [ratio estimation by $^{31}P\{^1H\}$ NMR resonance integration]. $^{31}P\{^1H\}$ NMR (121.5 MHz, CH_2Cl_2): δ = 183.0 [s_{sat}, $^1J_{W,P}$ = 254.3 Hz, **A** (9%)], 176.2 [s_{sat}, $^1J_{W,P}$ = 277.2 Hz, **B** (3%)], 172.5 [s_{sat}, $^1J_{W,P}$ = 309.0 Hz, **C** (6%)], 126.1 [**D** (1%)], 110.7 [**E** (1%)], 95.5 [s_{sat}, $^1J_{W,P}$ = 277.2 Hz, **F** (3%)], 54.4 [s_{sat}, $^1J_{W,P}$ = 270.8 Hz, **G** (1%)], 40.0 [**H** (1%)], –110.4 [s_{sat}, $^1J_{W,P}$ = 295.0 Hz, **1** (69%)] ppm. $^{19}F\{^1H\}$ NMR: δ = –134.0 (m_c, **2h**), –144.7 (m_c, **2h**), –160.6 (m_c, **2h**) ppm.

Theoretical Methods: DFT calculations were carried out with the TURBOMOLE V5.8 program package.[24] For optimizations the gradient corrected exchange functional by Becke[25] (B88) in combination with the gradient corrected correlation functional by Lee, Yang, and Parr[26] (LYP) with the RI approximation[27] and the valence-double-ζ basis set SV(P)[28] was used. For tungsten the effective core potential ECP-60-MWB[29] derived from the Stuttgart-Dresden group was used. The influence of the polar solvent was taken into account by employing the COSMO approach[30] with ε = 8.93. For cavity construction the atomic radii of Bondi[31] were used, which are obtained from crystallographic data. For tungsten the atomic radius was set to 2.2230 Å. The stationary points were characterized by numerical vibrational frequencies calculations by using the SNF 3.3.0 program package.[32] Single point calculations were carried out by using the Three Parameter Hybrid Functional Becke3[33] (B3) in combination with the LYP correlation functional[26] and the valence-triple-ζ basis set TZVP[34] and ECP-60-MWB for tungsten.

Supporting Information (see footnote on the first page of this article): Relative energies, enthalpies, and free energies for the reactions depicted in Schemes 4 and 5.

Acknowledgments

We are grateful to the Deutsche Forschungsgemeinschaft, the Fonds der Chemischen Industrie (Kekulé Stipendium for H. H.), the SFB 624 "Template", the John von Neumann Institute for Computing (HBN12), and Prof. Dr. B. Engels for computing time. A. E. wishes to acknowledge the grants from MEC-Spain (CTQ 2004–02201) and Fundación Séneca (CARM-Spain) (02970/PI/05). We thank G. von Frantzius for fruitful discussions.

[1] M. Schmittel, A. Burghart, *Angew. Chem.* **1997**, *109*, 2658–2699; *Angew. Chem. Int. Ed. Engl.* **1997**, *36*, 2550–2589.
[2] E. Baciocchi, M. Bietti, O. Lanzalunga, *Acc. Chem. Res.* **2000**, *33*, 243–251.
[3] M. Mella, M. Fagnoni, M. Freccero, A. Albini, *Chem. Soc. Rev.* **1998**, *27*, 81–89.
[4] A. A. Fokin, P. R. Schreiner, *Chem. Rev.* **2002**, *102*, 1551–1593.
[5] N. G. Connelly, W. E. Geiger, *Chem. Rev.* **1996**, *96*, 877–910.
[6] C. Gaebert, J. Mattay, M. Toubartz, S. Steenken, B. Müller, T. Bally, *Chem. Eur. J.* **2005**, *11*, 1294–1304.
[7] K. E. Torraca, L. McElwee-White, *Coord. Chem. Rev.* **2000**, *206–207*, 469–491.

[8] For example, see: U. Jahn, P. Hartmann, *Chem. Commun.* **1998**, 209–210, and references cited therein.
[9] T. Ramnial, I. McKenzie, B. Gorodetsky, E. M. W. Tsang, J. A. C. Clyburne, *Chem. Commun.* **2004**, 1054–1055.
[10] a) R. Streubel, A. Kusenberg, J. Jeske, P. G. Jones, *Angew. Chem.* **1994**, *106*, 2564–2566; *Angew. Chem. Int. Ed. Engl.* **1994**, *33*, 2427–2429; b) R. Streubel, J. Jeske, P. G. Jones, R. Herbst-Irmer, *Angew. Chem.* **1994**, *106*, 115–117; *Angew. Chem. Int. Ed. Engl.* **1994**, *33*, 80–82; c) R. Streubel, A. Kusenberg, *Phosphorus Sulfur Relat. Elem.* **1994**, *93–94*, 281–284; d) R. Streubel, A. Ostrowski, S. Priemer, U. Rohde, J. Jeske, P. G. Jones, *Eur. J. Inorg. Chem.* **1998**, 257–261.
[11] a) F. G. N. Cloke, P. B. Hitchcock, J. F. Nixon, U. Schiemann, R. Streubel, D. J. Wilson, *Chem. Commun.* **2000**, 1659–1660; b) H. Wilkens, A. Ostrowski, J. Jeske, F. Ruthe, P. G. Jones, R. Streubel, *Organometallics* **1999**, *18*, 5627–5642; c) R. Streubel, H. Wilkens, P. G. Jones, *Chem. Commun.* **1999**, 2127–2128; d) H. Wilkens, F. Ruthe, P. G. Jones, R. Streubel, *Chem. Eur. J.* **1998**, *4*, 1542–1553; e) R. Streubel, H. Wilkens, A. Ostrowski, C. Neumann, F. Ruthe, P. G. Jones, *Angew. Chem.* **1997**, *109*, 1549–1550; *Angew. Chem. Int. Ed. Engl.* **1997**, *36*, 1492–1493.
[12] R. Streubel, H. Wilkens, P. G. Jones, *Chem. Eur. J.* **2000**, *6*, 3997–4000.
[13] a) R. Streubel, C. Neumann, P. G. Jones, *J. Chem. Soc. Dalton Trans.* **2000**, 2495–2496; b) C. Neumann, E. Ionescu, U. Schiemann, M. Schlenker, M. Bode, F. Ruthe, P. G. Jones, R. Streubel, *J. Organomet. Chem.* **2002**, *643–644*, 253–264; c) C. Neumann, A. Prehn Junquera, C. Wismach, P. G. Jones, R. Streubel, *Tetrahedron* **2003**, *59*, 6213–6220.
[14] The numbering of atoms in heterocyclic complexes **3a**–**h** according to the Hantzsch-Widmann-Patterson nomenclature is used in this paper.
[15] P. W. Atkins, *Physical Chemistry*, 5th ed., Oxford University Press, Oxford, **1994**.
[16] Cyclovoltammetric measurements did not reveal conclusive results.
[17] M. A. Alvarez, G. García, M. E. García, V. Riera, M. A. Ruiz, *Organometallics* **1999**, *18*, 4509–4517.
[18] The ease of electrophilic aromatic substitution increases in the order: thiophene < furane < pyrrol. For example, see: D. T. Davies, *Aromatic Heterocyclic Chemistry*, Oxford University Press, Oxford, **1992**.
[19] X-ray crystallographic analysis of **3d**: Suitable yellow single crystals of **3d** were obtained from a concentrated *n*-pentane solution upon decreasing the temperature from ambient temperature to +4 °C. Data were collected with a Nonius KappaCCD diffractometer equipped with a low-temperature device (Cryostream, Oxford Cryosystems) at 123 K by using graphite monochromated Mo-K_α radiation (λ = 0.71073 Å). The structure was solved by Patterson methods (SHELXS-97)[20a] and refined by full-matrix least-squares on F^2 (SHELXL-97).[20b] All non-hydrogen atoms were refined anisotropically. The hydrogen atoms were included isotropically by using the riding model on the bound atoms. The thiophene substituent is disordered [occupancy: 0.81(1): 0.19(1)]. Semiempirical absorption correction was carried out from equivalents (min./max. transmissions = 0.27295/0.61685). $C_{24}H_{27}N_2O_5PSSi_2W$; crystal size 0.45 × 0.30 × 0.12 mm, triclinic, $P\bar{1}$ (No.2), a = 10.9114(2) Å, b = 12.1675(2) Å, c = 13.1114(2) Å, α = 96.695(1)°, β = 110.108(1)°, γ = 109.554(1)°, V = 1486.63(4) Å^3, Z = 2, $\rho_{calcd.}$ = 1.623 Mg m^{-3}, $2\theta_{max}$ = 55°, collected (independent) reflections = 14224 (6590), R_{int} = 0. 0716, μ = 4.124 mm^{-1}, 318 refined parameters, 51 restraints, R_1 [for $I > 2\sigma(I)$] = 0. 0361, wR_2 (for all data) = 0.0935, max./min. residual electron density = 2.745/–3.017 e Å^{-3}. X-ray crystallographic analysis of **3b**, **3e**: Crystals were obtained from a concentrated *n*-pentane solution. Data were collected with a Bruker SMART 1000 CCD diffractometer equipped with a low-temperature device. Structure solution and refinement as above. **3b**: $C_{26}H_{32}N_3O_5PSi_2W$; crystal size 0.19 × 0.14 × 0.06 mm, triclinic, $P\bar{1}$ (No.2), a = 10.823(2) Å, b = 12.207(2) Å, c = 13.395(3) Å, α = 96.101(6)°, β = 110.126(6)°, γ = 107.666(6)°, V = 1538.7(5) Å^3, Z = 2, $\rho_{calcd.}$ = 1.592 Mg m^{-3}, $2\theta_{max}$ = 60°, collected (independent) reflections = 30876 (8933), R_{int} = 0.0501, μ = 3.92 mm^{-1}, 351 refined parameters, 63 restraints, R_1 [for $I > 2\sigma(I)$] = 0. 0451, wR_2 (for all data) = 0.1125, max./min. residual electron density = 3.80/–5.13 e Å^{-3}. **3e**: $C_{24}H_{27}N_2O_5PSSi_2W$; crystal size 0.35 × 0.23 × 0.16 mm, triclinic, $P\bar{1}$ (No. 2), a = 10.8501(12) Å, b = 12.2138(12) Å, c = 13.1138(14) Å, α = 96.171(3)°, β = 110.016(3)°, γ = 110.191(3)°, V = 1481.5(3) Å^3, Z = 2, $\rho_{calcd.}$ = 1.629 Mg m^{-3}, $2\theta_{max}$ = 61°, collected (independent) reflections = 24334 (8967), R_{int} = 0. 0250, μ = 4.14 mm^{-1}, 331 refined parameters, 31 restraints, R_1 [for $I > 2\sigma(I)$] = 0. 0179, wR_2 (for all data) = 0.0455, max./min. residual electron density = 1.417/–1.308 e Å^{-3}. CCDC-646819 (for **3b**), -639472 (for **3d**), and -646820 (for **3e**) contain the supplementary crystallographic data for this paper. These data can be obtained free of charge from The Cambridge Crystallographic Data Centre via www.ccdc.cam.ac.uk/data_request/cif.
[20] a) SHELXS-97: G. M. Sheldrick, *Acta Crystallogr., Sect. A* **1990**, *46*, 467–473; b) G. M. Sheldrick, SHELXL-97, University of Göttingen, **1997**.
[21] H. Helten, T. Schirmeister, B. Engels, *J. Phys. Chem. A* **2004**, *108*, 7691–7701.
[22] R. Streubel, *Top. Curr. Chem.* **2002**, *223*, 91–101.
[23] The model reaction using **4** and H_2NCN may be representative for the reaction of **1** with Me_2NCN (**2a**), but also for the reactions with the electron-rich five-membered heterocyclic nitrile derivatives **2b**–**e**.
[24] TURBOMOLE V5.8: see http://www.cosmologic.de/Quantum-Chemistry/ main_turbomole.html.
[25] A. D. Becke, *Phys. Rev. A* **1988**, *38*, 3098–3100.
[26] C. Lee, W. Yang, R. G. Parr, *Phys. Rev. B* **1988**, *37*, 785–789.
[27] a) K. Eichkorn, O. Treutler, H. Öhm, M. Häser, R. Ahlrichs, *Chem. Phys. Lett.* **1995**, *240*, 283–290; b) K. Eichkorn, O. Treutler, H. Öhm, M. Häser, R. Ahlrichs, *Chem. Phys. Lett.* **1995**, *242*, 652–660; c) K. Eichkorn, F. Weigend, O. Treutler, R. Ahlrichs, *Theor. Chem. Acc.* **1997**, *97*, 119–124.
[28] A. Schäfer, H. Horn, R. Ahlrichs, *J. Chem. Phys.* **1992**, *97*, 2571–2577.
[29] D. Andrae, U. Häußermann, M. Dolg, H. Stoll, H. Preuß, *Theor. Chim. Acta* **1990**, *77*, 123–141.
[30] A. Klamt, G. Schürmann, *J. Chem. Soc. Perkin Trans. 2* **1993**, 799–805.
[31] A. Bondi, *J. Phys. Chem.* **1964**, *68*, 441–451.
[32] J. Neugebauer, M. Reiher, C. Kind, B. A. Hess, *J. Comput. Chem.* **2002**, *23*, 895–910.
[33] A. D. Becke, *J. Chem. Phys.* **1993**, *98*, 5648–5652.
[34] A. Schäfer, C. Huber, R. Ahlrichs, *J. Chem. Phys.* **1994**, *100*, 5829–5835.

Received: June 27, 2007
Published Online: August 22, 2007

